THE ASTRONOMICAL JOURNAL VOLUME 71, NUMBER 1 FEBRUARY 1966

# The Structure of Star Clusters. III. Some Simple Dynamical Models

IVAN R. KING
*Berkeley Astronomy Department, University of California*

(Received 20 October 1965)

Dynamical models of star clusters are presented, based on steady-state solutions of the Fokker–Planck equation. The models are spatially limited, corresponding to the tidal cutoff imposed by the Milky Way. Their projected density distributions are similar to those observed in open clusters, globular clusters, and elliptical galaxies. Within each model the fractional escape rate is uniform throughout. The escape rate from a cluster depends on the number of stars and the strength of the tidal force field; when expressed in this way it is almost independent of core radius or central concentration. Quantitative application to actual clusters must await a discussion of models containing a realistic stellar mixture.

## I. INTRODUCTION

IN the 50-yr history of dynamical studies of star clusters a number of basic points have become clear. First, the theory of stellar encounters has shown [Chandrasekhar 1960, Eq. (5.227)] that the mean free path in a star cluster is many times the radius of the cluster. Spatial mixing is therefore much more effective than relaxation through stellar encounters, and one may expect the structure of a star cluster to be closely represented by a solution of the encounterless Liouville equation, with stellar encounters producing a slow evolution from one such solution to another.

The general solution of the steady-state encounterless Liouville equation was given long ago by Jeans (1915): The distribution function in phase space must be expressible as a function of the isolating integrals of the equations of motion of a star. For the case of spherical symmetry in position space the only known isolating integrals for a general potential function $V(r)$ are the energy and angular momentum per unit mass,

$$E=\tfrac{1}{2}v^2+V(r), \tag{1}$$

$$h=rv_t, \tag{2}$$

where $v$ is the magnitude of the velocity and $v_t$ is its tangential component. Even so, Jeans' theorem leaves possible a very wide range of cluster models. One needs only to glance at actual clusters, however, to see the strong similarity between one cluster and another; and indeed, Paper I of this series (King 1962) has shown that the similarity between clusters is as strong as external circumstances will allow it to be. The actual clusters clearly prefer a particular set of distribution functions, and it should be the task of the theory to find and describe that set.

Since the time of relaxation at the center of a globular cluster is a small fraction of its age [see, for instance, Oort and van Herk (1959)], it is natural to look to stellar encounters to provide the regularizing mechanism in star clusters. One may approach the problem by asking that stellar encounters determine a velocity distribution, which then determines the spatial characteristics of the model. This approach has been used by many investigators (Chandrasekhar 1960, p. 231; Woolley 1954; Woolley and Robertson 1956; Woolley and Dickens 1961; Spitzer and Härm 1958; Oort and van Herk 1959; Michie 1963a,b; Michie and Bodenheimer 1963), each of whom chose a somewhat different velocity distribution. The discussion that follows can be considered to be an extension of the work of Chandrasekhar and of Spitzer and Härm.

As a start, consider the ideal but unattainable equilibrium distribution, a Gaussian velocity distribution. This is easily shown (Chandrasekhar 1960, p. 231) to lead to a density distribution that corresponds to the isothermal gas sphere. This model has a total mass that is strongly infinite; when $r$ is large, the mass contained within a radius $r$ increases in direct proportion to $r$. In fact, the Gaussian velocity distribution could have been rejected *a priori*; for a cluster cannot retain stars whose velocity exceeds a finite escape velocity. What is needed is a velocity distribution that will be produced by stellar encounters yet drops to zero at a finite limiting velocity. The mechanism for solving this problem was provided by Chandrasekhar (1943a), who introduced the Fokker–Planck equation into stellar dynamics to calculate the effect of encounters on a velocity distribution. To describe the velocity distribution in a star cluster he found a steady-state solution of the Fokker–Planck equation with a finite cutoff velocity (Chandrasekhar 1943b). He used this solution only to determine the rate of escape of stars, however, and did not give the velocity distribution explicitly.

The problem was taken up later by Spitzer and Härm (1958), who tabulated the steady-state velocity distribution and incidentally corrected an error of a factor of 2 in Chandrasekhar's escape rate. Spitzer and Härm attempted to use their steady-state velocity distribution to derive a cluster model, but in this attempt they were disappointed. No matter what they chose for the central value of the potential, the density in their model went to zero at some finite value of the radius, contradicting their identification of the cutoff velocity with the escape velocity from the cluster.

## II. SPATIALLY LIMITED MODELS

Recent observational results suggest a re-examination of the difficulties encountered by Spitzer and Härm.

It has been shown both theoretically (von Hoerner 1957) and observationally (King 1962) that a star cluster is not unlimited in extent; a finite boundary is set by the tidal force of the Milky Way. The velocities at any point in the cluster will then be correspondingly limited, the highest velocity being that needed to reach the cluster boundary—not the velocity of escape to infinity. This is exactly the situation in the model calculated by Spitzer and Härm, which thus appears to be a valid model for a tidally limited cluster. The change is one of interpretation; "escape" now means passing beyond the boundary of the cluster, since any star that does so is quickly lost in the tidal force field.

Spitzer and Härm gave a cluster model for only one value of the cutoff velocity, but different cutoffs will give rise to other models with different limiting radii. To calculate each model two steps are required: (1) solving the steady-state Fokker–Planck equation and (2) converting the resulting velocity distribution into a spatial model. The Fokker–Planck solutions are given numerically in Paper II of this series (King 1965). It is shown there that those velocity distributions are well represented by Michie's (1963a) approximation, which is simply the Maxwellian distribution function minus a constant.

Although the basic method is clear, two problems stand between the chosen velocity distribution and its application to actual globular clusters. First, the assumed velocity distribution at the cluster center contains no information about anisotropy of velocities in the outer parts of the cluster. Second, a real cluster is a mixture of stars, each type having a different mass and a different spatial distribution. Anisotropy and mixture will both affect the details of any cluster model; nevertheless, the basic physical properties of star clusters follow from the existence of a relaxed velocity distribution in a spatially limited configuration. The present paper therefore confines itself to the simplest of models, in which the stars all have the same mass and the velocity distribution is everywhere isotropic. The models given here represent, therefore, only a small step forward from the gross empiricism of Paper I; and their properties are discussed in a general rather than a quantitative way. Later papers will fit mixed models to actual clusters and will explore the problems of anisotropy.

## III. CALCULATION OF MODELS

To build a cluster model we start by choosing a velocity distribution at the center of the cluster, where relaxation is fastest. As previously suggested, let the distribution function of position and velocity at this point be

$$f(0,v)=k[\exp(-j^2v^2)-\exp(-j^2v_e^2)], \tag{3}$$

where $v_e$ is the escape velocity. The energy integral for a star is

$$E=\tfrac{1}{2}v^2+V(r). \tag{4}$$

Let $V$ be zero at the surface of the cluster; zero energy then corresponds to an ability barely to reach the surface. The escape velocity at any point is thus given by

$$v_e^2=-2V. \tag{5}$$

Above zero energy $f(v)$ is taken to be zero, since stars of positive energy are removed by the tidal forces. Tidal distortion of the cluster shape is neglected; it affects only the outermost regions and can in principle be taken into account later as a perturbation.

In terms of $E$, the distribution function at the center of the cluster is

$$f(0,v)=k\exp(2j^2V_0)[\exp(-2j^2E)-1]. \tag{6}$$

But, according to Jeans' theorem the distribution function must be the same function of $E$ at all points; hence at any other point the distribution function is, according to Eqs. (4)–(6),

$$f(r,v)=k\exp[-2j^2(V-V_0)] \times[\exp(-j^2v^2)-\exp(-j^2v_e^2)], \tag{7}$$

where $v_e$ is now the value given by Eq. (5) for the point under consideration. Eq. (7) is extremely gratifying, since the velocity distribution has the same form as that in Eq. (3). In other words, to the accuracy of the Michie approximation, the velocity distribution at *every* point in the cluster is the appropriate steady-state solution of the Fokker–Planck equation, for the velocity cutoff that correctly applies at that point. Stellar encounters are thus automatically taken into account *everywhere* in the cluster, not just at the center.

The density at any point can now be found by integrating $f(r,v)$ with respect to velocity:

$$\rho=\int_0^{v_e} f(r,v)4\pi v^2dv. \tag{8}$$

With Eq. (7) and the substitutions

$$W=-2j^2V, \tag{9}$$

$$\eta=j^2v^2, \tag{10}$$

this becomes

$$\begin{aligned}\rho&=2\pi kj^{-3}\exp(W-W_0)\int_0^W(e^{-\eta}-e^{-W})\eta^{\frac{1}{2}}d\eta\\&=\tfrac{4}{3}\pi kj^{-3}\exp(W-W_0)\int_0^W e^{-\eta}\eta^{\frac{3}{2}}d\eta,\end{aligned} \tag{11}$$

the last step being an integration by parts. Unfortunately $\rho$ is given as a function not of $r$ but of $W$. Its dependence on $r$ can be found only by solving Poisson's

equation,

$$\frac{d^2V}{dr^2}+\frac{2}{r}\frac{dV}{dr}=4\pi G\rho. \tag{12}$$

In terms of $W$ and a dimensionless radius

$$R=r/r_c, \tag{13}$$

this is

$$\frac{d^2W}{dR^2}+\frac{2}{R}\frac{dW}{dR}=-8\pi G j^2 r_c^2\rho. \tag{14}$$

Substitution of power series for the variables shows that the scale factor $r_c$ will be very close to the "core radius" in the empirical formula of Paper I, provided the central value of $\nabla^2 W$ is taken to be $-9$. Thus

$$8\pi G j^2 r_c^2\rho_0=9, \tag{15}$$

and

$$\frac{d^2W}{dR^2}+\frac{2}{R}\frac{dW}{dR}=-9\frac{\rho}{\rho_0}, \tag{16}$$

so that only relative values of the density are needed.

In the actual computation the first step was to tabulate the quantity

$$\Psi=e^W\int_0^W e^{-\eta}\eta^{\frac{1}{2}}d\eta, \tag{17}$$

which is proportional to the density. A model could then be computed by choosing a value of $W_0$, the central value of $W$. The ratio $\rho/\rho_0$ was formed for all values of $W$, and Poisson's equation was solved starting at $R=0$. The other initial condition needed is $dW/dR=0$ at $R=0$; substitution of power series in Eq. (16) shows that this implies

$$\lim_{R\to 0}\frac{2}{R}\frac{dW}{dR}=-6. \tag{18}$$

This procedure has the advantage of being completely straightforward: the surface occurs at the value of $R$ where $W$ (and hence $\rho$) reaches zero, and every integration of Poisson's equation leads to a valid model. The larger the value of $W_0$, the larger is the surface radius; as $W_0\to\infty$ the velocity distribution approaches Maxwellian, the surface radius increases without limit, and the model approaches the isothermal sphere.

The final step in the computation was to project the spatial densities onto the plane of the sky, for comparison with observation. This is far preferable to converting the observational results to space densities, since the conversion process would greatly magnify the observational errors.

Several points are worth noting with regard to the computational procedure:

(1) The quadrature in Eq. (17) is difficult to carry out in that form, since the second and higher derivatives of $\eta^{\frac{1}{2}}$ are infinite at the lower limit. The integral was therefore evaluated in the form

$$\int_0^{W^{\frac{1}{2}}}\exp(-x^2)x^4dx,$$

which is just $\frac{1}{2}$ times the integral in Eq. (17).

(2) The density $\rho$ was available for specific values of $W$ rather than specific values of $R$. The differential equation was therefore transformed so as to make $R$ the dependent and $W$ the independent variable.

(3) Since $R$ becomes very large in some models, $1/R$ was used instead in the outer parts. Near the center $R$ was replaced by $R^2$. The equations used were

$$-X\frac{d^2X}{dW^2}+\frac{3}{2}\left(\frac{dX}{dW}\right)^2=-\frac{9}{4}\frac{\rho}{\rho_0}\left(\frac{dX}{dW}\right)^3, \tag{19}$$

$$\frac{d^2P}{dW^2}=9\frac{\rho}{\rho_0}\frac{1}{P^4}\left(\frac{dP}{dW}\right)^3, \tag{20}$$

where

$$X=R^2, \tag{21}$$

$$P=1/R. \tag{22}$$

(4) The surface density, projected on the plane of the sky, is

$$\begin{aligned}\sigma(R)&=2\int_R^{R_t}\frac{\rho(S)SdS}{(S^2-R^2)^{\frac{1}{2}}}\\&=\int_X^{X_t}\frac{\rho dY}{(Y-X)^{\frac{1}{2}}},\end{aligned} \tag{23}$$

where $X=R^2$, $Y=S^2$, and subscript $t$ refers to values at the surface. This quadrature is awkward in two ways: the upper limit can be very large, and the integrand is infinite at the lower limit. The upper limit was therefore normalized by making the transformation

$$t=\frac{Y-X}{1+Y}, \tag{24}$$

so that

$$\sigma(R)=\frac{1}{1+X}\int_0^1(1+Y)^{\frac{1}{2}}\rho t^{-\frac{1}{2}}dt, \tag{25}$$

where

$$Y=(t+X)/(1-t). \tag{26}$$

The upper limit has been extended to $Y=\infty$, so that $\rho$ must be taken to be zero beyond $Y=Y_t$. The difficulty at the lower limit was handled by using the quadrature formula

$$\begin{aligned}&\int_0^{t_1}\varphi(t)t^{-\frac{1}{2}}dt\\&=\frac{4}{15}t_1^{\frac{1}{2}}\left[\left(5-\frac{t_1}{t_2}\right)\varphi_0+\frac{3t_1-5t_2}{2(t_1-t_2)}\varphi_1+\frac{t_1^2}{t_2(t_1-t_2)}\varphi_2\right]\end{aligned} \tag{27}$$

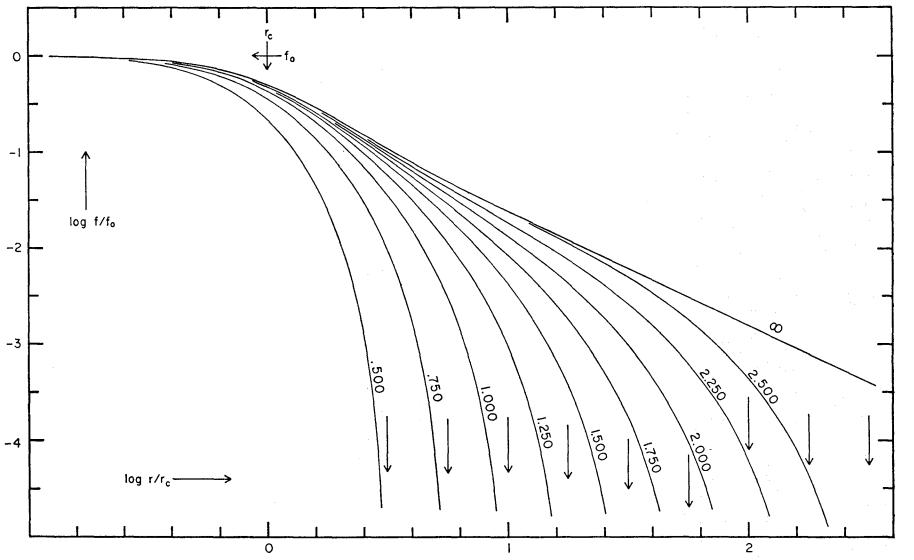


FIG. 1. Surface densities in single-mass models. Arrows indicate $\log r_t$. These curves may be used directly with inch graph paper.

for the first integration step. This formula fits a second-degree polynomial to values of $\varphi$ at $t=0$, $t_1$, and $t_2$ and absorbs the awkward factor $t^{-\frac{1}{2}}$ into the integration.

(5) Fifty steps in $W$ were found to give adequate precision. A Fortran program run on an IBM 7094 produced nine models per minute. The major expenditure of computing time was in the projection process.

## IV. RELATION TO ACTUAL CLUSTERS

The resulting models are modifications of the isothermal sphere. Near the center their densities are very close to isothermal, but eventually they fall below the isothermal curve and drop to zero. The projected densities are shown in Fig. 1, where the surface density is called $f$ and the units of $f$ and $r$ are the central value $f_0$ and the core radius $r_c$, respectively. The curves are labeled with values of $\log r_t/r_c$. For easy comparison with observations the figure has been printed on such a scale that the horizontal and vertical units are exactly 1.25 and 0.5 inches.

The curves of Fig. 1 supersede the purely empirical curves given in Fig. 5 of Paper I (King 1962). In the range $W_0 \leq 7$, which is the range covered by the observational checks in Paper I, they agree closely with the empirical family of curves and fit the observations equally well. Examples of the observational fit in high and low-concentration clusters are shown in Figs. 2 and 3. The data are star counts on plates taken with the 48-in. Palomar Schmidt. The vertical lines indicate statistical mean errors, according to the Poisson distribution. (In Fig. 2 the value of $r_c$ is not shown,

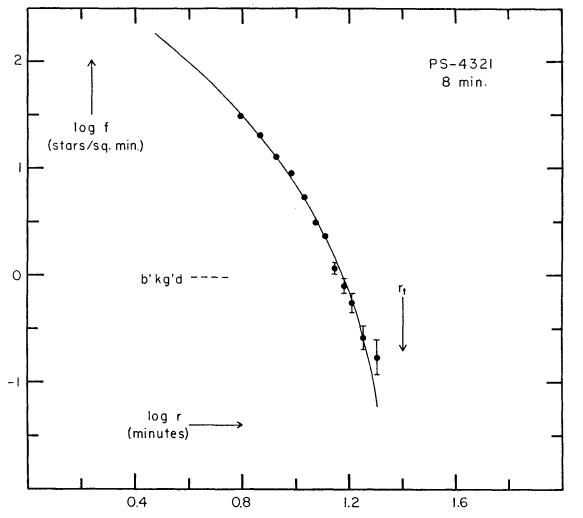


FIG. 2. Comparison of star counts in M13 with theoretical curve for $\log(r_t/r_c)=1.50$. Maximum-exposure 48-in. Schmidt plate.

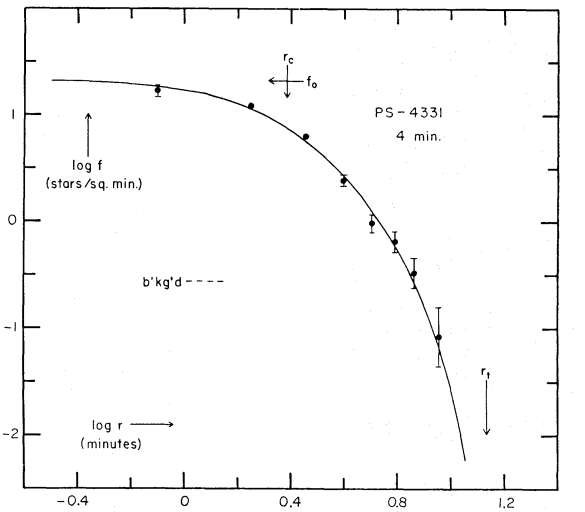


FIG. 3. Comparison of star counts in NGC 5053 with theoretical curve for $\log(r_t/r_c)=0.75$. Medium-exposure 48-in. Schmidt plate.

since for these exterior counts the fitting is rather insensitive to the value chosen for the core radius. The value used for $r_c$ was, in fact, determined from photoelectric surface photometry.)

For higher values of $W_0$ the theoretical and empirical curves differ, in that the theoretical curves go through an inflection and thereafter have an asymptotic slope of $-1$ rather than $-2$. This difference does not, however, indicate a disagreement between theory and observation. The central concentrations involved are in fact higher than those observed in any star cluster; hence the "empirical" curves in this range were not based on fact but rather on a misguided extrapolation. To study such high central concentrations observationally we must examine the elliptical galaxies, whose brightness profiles were found in Paper I to disagree with the high-concentration extrapolation of the empirical curves. When comparison is made instead with the theoretical family illustrated in Fig. 1, the answer is very different. Figure 4 shows a comparison with the photoelectric observations of Miller and Prendergast (1962) in NGC 3379—the most reliable study yet made of surface brightnesses in an elliptical galaxy. Most of the points are directly measured surface brightnesses in yellow light, but a few have been converted from blue measures. The ellipticity has been compensated by reducing all distances along the $E$–$W$ line by $\Delta \log r = 0.025$ and increasing all distances along the $N$–$S$ line by the same factor. In the central regions the angular resolving power of the photometer apertures is too low to sketch a brightness profile directly; instead central magnitudes measured through concentric apertures of various sizes have been converted to local surface brightnesses.

It is clear from Fig. 4 that a star-cluster profile approximates the observed distribution of light in NGC 3379. Such a similarity is surprising, however; for the cluster profiles have been shown to result from relaxation, while the relaxation time in NGC 3379 is longer than $10^{12}$ yr. It was suggested in Paper I that an alternative and much more rapid relaxation may have taken place in the initial settling down of the system. The tidal limitation could then be imposed at any later time; the only requirement for the present models is that the cutoff be imposed on energies rather than positions—which is indeed a characteristic of a tidal force. (Strictly, the cutoff in these models should also be gradual rather than sharp; but the difference—discussed in the following section—would be very difficult to observe in the faint outer envelope of an elliptical galaxy.)

The comparison with observation need not be pressed further here; the important point is that star clusters and spherical galaxies both resemble cluster

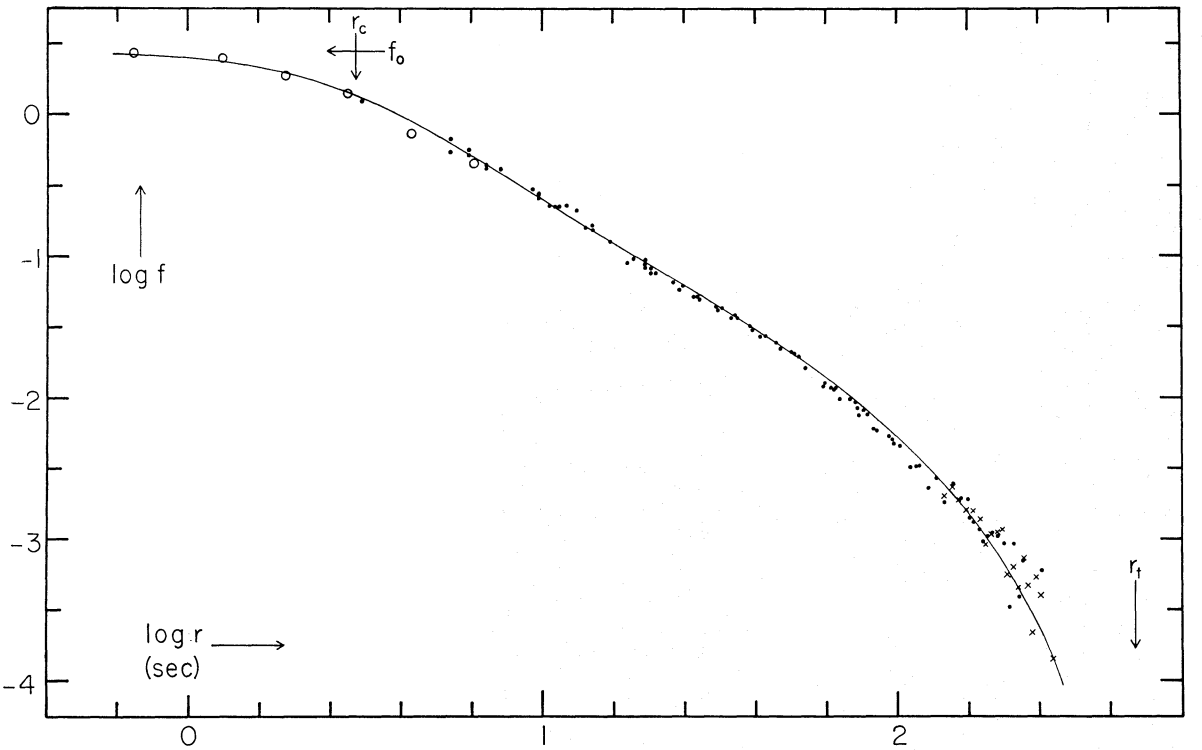


FIG. 4. Comparison of surface brightnesses in NGC 3379 with theoretical curve for $\log(r_t/r_c) = 2.20$. Ordinate: logarithm of yellow surface brightness (unit is $16^m.91$/sq sec); abscissa: logarithm of radius in seconds. Open circles are values calculated from concentric circular measurements, dots are point measurements in the yellow, and crosses are blue measurements converted by assuming $B-V = 0.96$.

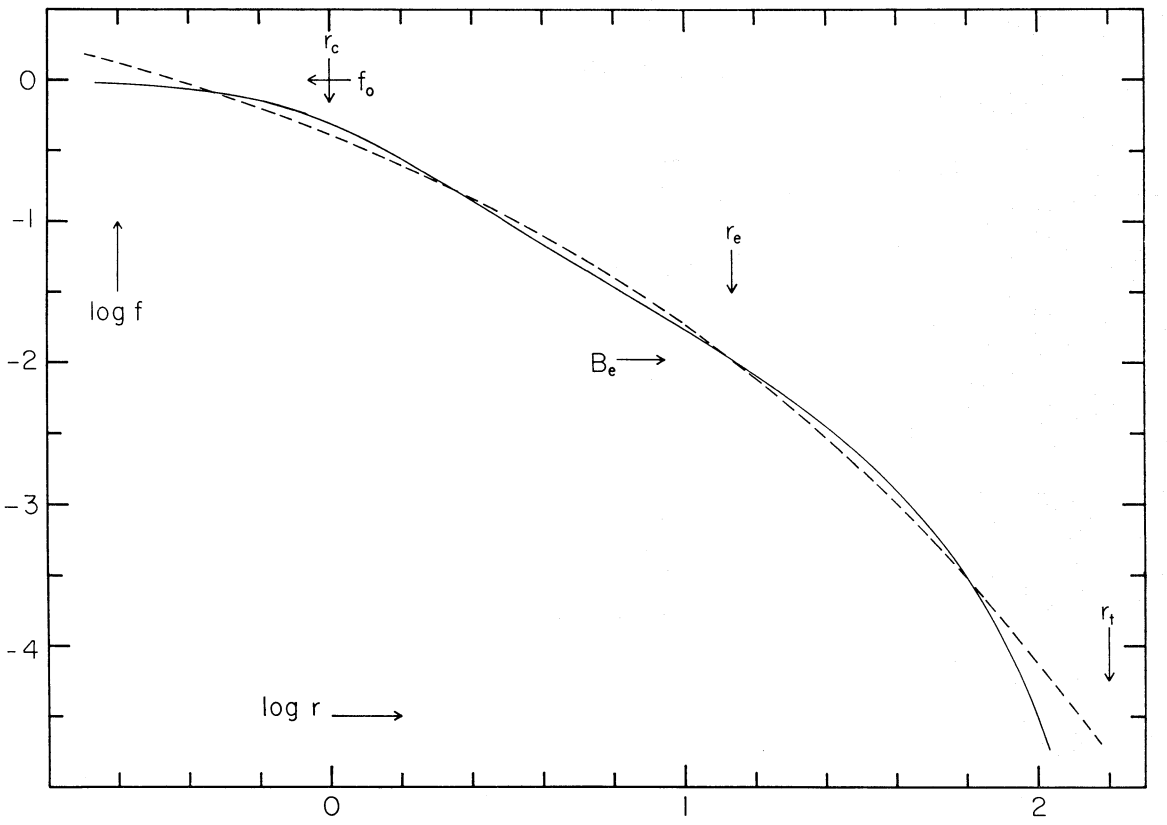


FIG. 5. Comparison between de Vaucouleurs' law and a modified isothermal model. Characteristic parameters of each curve are marked.

models of the sort described here. Conservatively then, the models at least provide a convenient set of interpolating curves; and with a shade more boldness one may expect the theoretical models to share some of the dynamical characteristics of real stellar systems.

A final point in this observational discussion is a comparison with de Vaucouleurs' law (1959), which has been suggested as a general law for surface brightnesses in elliptical galaxies. Figure 5 shows de Vaucouleurs' law, along with the modified isothermal model that has $\log(r_t/r_c)=2.20$. The region covered by existing observations of elliptical galaxies is roughly $0\leq\log(r_t/r_c)\leq 2$; over this range the two curves are quite similar. In the light of the present discussion, de Vaucouleurs' law appears to refer to a particular central concentration and should be appropriate only for galaxy profiles that have that concentration. For lower central concentrations, in fact, de Vaucouleurs' law is known to fit poorly (Hodge 1961a, b, 1962, 1964; Rood 1965). Furthermore, de Vaucouleurs' law does not appear to fit the center of any stellar system.

## V. COMPARISON WITH OTHER MODELS

Many of the characteristics of the models described here follow from the mere fact that their velocity distributions are nearly Gaussian. At the same time their appearance must depend in some way on the exact nature of the non-Gaussian deviations. One question is the shape of the velocity cutoff. Steady-state relaxation theory predicts a distribution that drops to zero continuously with finite slope, but arguments have also been presented for a distribution that is truncated at the cutoff velocity (Woolley 1961; Woolley and Dickens 1961). To examine such models the computations of Sec. III were repeated for a truncated Gaussian distribution. In that case the first form of Eq. (11) lacks the quantity $e^{-W}$ in the integrand, and Eq. (17) is replaced by

$$\Psi=e^{W}\int_0^W e^{-\eta}\eta^{\frac{1}{2}}d\eta, \tag{28}$$

where a constant numerical factor has again been dropped. By way of further exploration, still another set of models was calculated from a velocity distribution in which the cutoff is even more gradual than that of the steady-state distribution. This sort of cutoff can be achieved by subtracting from the Maxwellian $e^{-\eta}$ a function that makes both the distribution function and its derivative zero at $\eta=W$. For one such

function the relative densities are then given by

$$\rho = 2\pi k j^{-3} \exp(W - W_0) \times \int_0^W [e^{-\eta} - e^{-W}(1 + W - \eta)]\eta^{\frac{1}{2}} d\eta. \quad (29)$$

If the second term is integrated directly and the first term is integrated twice by parts, the result is

$$\rho = \frac{8}{15}\pi k j^{-3} \exp(W - W_0) \int_0^W e^{-\eta}\eta^{\frac{5}{2}} d\eta. \quad (30)$$

A full set of models was computed for each of these modified cutoffs. As expected, the central profiles were closely similar, the differences appearing only in the shape of the density dropoff near the spatial limit. A comparison for one value of $W_0$ is given in Fig. 6.

The models based on a truncated Maxwellian distribution are the same as those of Woolley and Dickens (1961). Their $k$ is the same as $W_0$ of this paper, while their linear variables $z$ and $a$ are equal to $3R$. Woolley has argued (1961) that the cutoff region of the velocity distribution contains too few stars to matter, but this contention is not borne out by Fig. 6, in which the curves separate widely within the region that is now covered by star counts on long-exposure plates. This difference is further illustrated by Fig. 7, in which the same count shown in Fig. 2 has been fitted with a curve from the family based on a truncated velocity distribution. The fit is significantly less good.

As a by-product of this manipulation of cutoffs, one can derive the variation of velocity dispersion with distance from the cluster center. With the steady-state velocity distribution, Eq. (7), it is easily found that the mean square velocity at any point is given by

$$\frac{\langle v^2 \rangle}{\langle v^2 \rangle_{W\to\infty}} = \frac{2}{5} \frac{\int_0^W e^{-\eta}\eta^{\frac{5}{2}} d\eta}{\int_0^W e^{-\eta}\eta^{\frac{3}{2}} d\eta}. \quad (31)$$

These integrals were tabulated in the course of the cluster-model computations; values of $\langle v^2 \rangle / \langle v^2 \rangle_{W\to\infty}$ are given in Table I.

A more serious change in the velocity distribution would be to give up the simplification of isotropy. Whether or not this is necessary is not at all clear; intuitive theoretical arguments can be given on either side. Against isotropy is the cosmogonic hypothesis that stars in the outer parts of a cluster have been ejected from the central regions and are therefore in predominantly radial orbits. Relaxation in the outer parts is too slow to change many of these into orbits of higher angular momentum. In favor of isotropy it may be argued that we do not know that the clusters were formed in this way. Furthermore the galactic

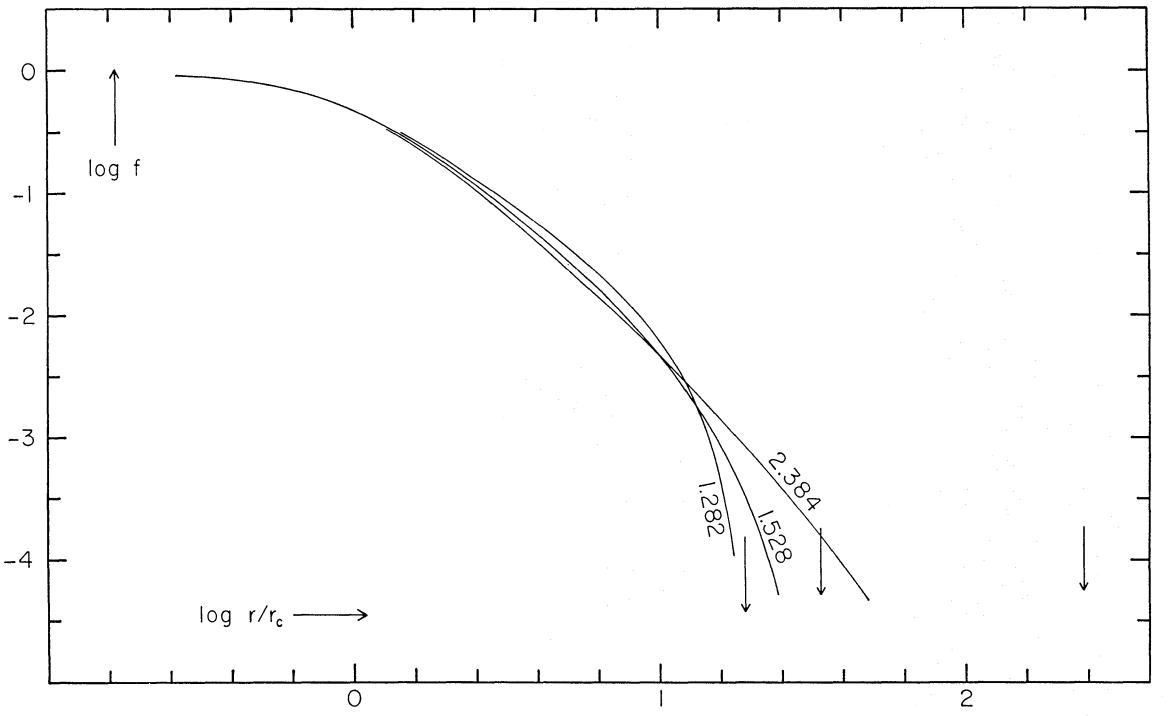


FIG. 6. Effect of velocity cutoff on surface densities. Left to right at bottom end, curves correspond to truncated, linear, and quadratic cutoffs, respectively.

tidal force, which strongly affects motions in the outer parts of a cluster, does not conserve angular momentum and can therefore be expected to randomize the distribution of angular momenta of outlying stars.

Michie and Bodenheimer have calculated a set of cluster models based on anisotropic velocity distributions (Michie 1963a; Michie and Bodenheimer 1963). Their models are spatially infinite, but the densities in the outer parts drop below that of the isothermal sphere because the velocity distribution becomes more and more radial. In a later paper (1963b) Michie adds the effect of a tidal cutoff. These limited models differ from those of the present paper in having an additional factor—anisotropy—that pulls the density down in the outer parts. In fitting to an observed cluster profile, part of the outer dropoff of density is therefore provided by the anisotropy; the tidal part of the dropoff is then correspondingly less severe, and a larger tidal limit is deduced. If the tidal limit were firmly known, the degree of anisotropy could be determined, but this is unfortunately not possible. Thus Paper I of this series

TABLE I. Effect of cutoff on mean-square velocity.

| $W$ | $\langle v^2\rangle/\langle v^2\rangle_{W\to\infty}$ | $W$ | $\langle v^2\rangle/\langle v^2\rangle_{W\to\infty}$ |
|---|---|---|---|
| 0.5 | 0.138 | 4.5 | 0.838 |
| 1.0 | 0.264 | 5.0 | 0.877 |
| 1.5 | 0.383 | 6.0 | 0.931 |
| 2.0 | 0.489 | 7.0 | 0.963 |
| 2.5 | 0.582 | 8.0 | 0.981 |
| 3.0 | 0.663 | 9.0 | 0.990 |
| 3.5 | 0.733 | 10.0 | 0.995 |
| 4.0 | 0.790 | | |

fits star counts in the galactic clusters NGC 7789 and M67 with models based on isotropic velocities; on the other hand Michie (1963b) chooses somewhat larger tidal limits and fits the same counts with models of rather marked velocity anisotropy. At best an upper limit can be set to the degree of anisotropy, based on the largest admissible value of the tidal limit. For the low central concentrations shown by galactic clusters this limit is very liberal, but it may be hoped that the higher central concentrations found among globular clusters will allow a better discrimination between tidal dropoff and anisotropy dropoff and thus allow a useful upper limit to be set on the anisotropy.

For effective comparison Michie's variables must be related to those of the present paper. To do this, Eq. (15) can be combined with Eq. (5.5) of Michie's Paper I (1963a) to show that the unit of Michie's radial variable $z$ is $(\pi^{\frac{1}{2}}/6)r_c$, or $0.222r_c$.

The most realistic of previously published models is that of Oort and van Herk (1959), which contains a mixture of stellar types. However, since the present paper considers only single-type models, discussion of their model will be deferred to a later paper, in which mixed models will be presented.

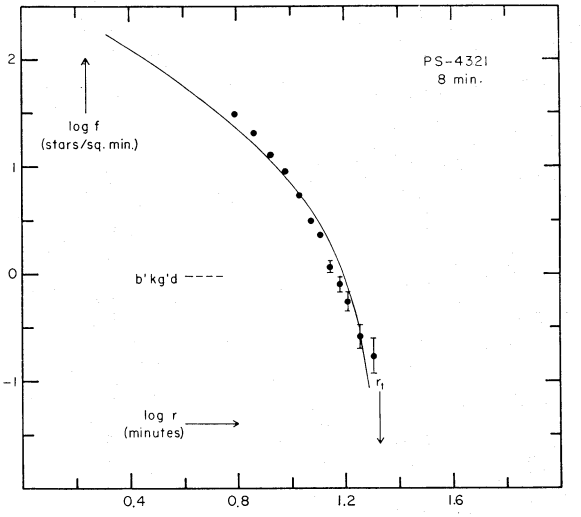


FIG. 7. Same star count as Fig. 2, fitted with a truncated velocity distribution.

## VI. ESCAPE RATE

Given a dynamical model of a star cluster, we can calculate the rate at which stars escape from the cluster. For actual clusters the models used should contain a realistic mixture of stellar types; hence calculation of actual escape rates is deferred to a later paper. The present simplified models can be used, however, to explore some basic questions concerning escape rates: (1) How does the escape rate depend on the parameters of the cluster model? (2) In a given model, how does the escape rate vary with position in the cluster? (3) How does the escape of stars cause the cluster to evolve?

The escape rate is implicit in the velocity distributions on which the models are based. These velocity distributions arose from a separation of variables in the time-dependent Fokker–Planck equation. To each velocity distribution corresponds an eigenvalue $\lambda$, which also appears in the time equation [cf. Eq. (5) of Paper II]:

$$-\frac{1}{\nu}\frac{d\nu}{dt}=\frac{\lambda}{T_R}. \tag{32}$$

Since we are no longer dealing with a system of constant density, $\nu$ is here taken to be the star density at a particular point of the cluster. At that point the fractional loss rate per unit time is given by Eq. (32), with the value of $\lambda$ that corresponds to the velocity distribution at that point. The time scale is given by the reference time

$$T_R=[2\pi G^2m^2\nu j^3\ln(\tfrac{1}{2}n)]^{-1}. \tag{33}$$

(The subscript zero of Paper II, which referred to stars of the dominant type, has been dropped here, where all stars are of a single type. In the present paper

subscript zero refers to values at the center of the cluster.)

In their basic study of velocity distributions Spitzer and Härm (1958) set the argument of the logarithm in Eq. (33) equal to half the total number of stars in the cluster, basing their choice on an implied argument that involves the application of the virial theorem to the whole cluster. In the present case, however, the use of a detailed dynamical model allows this choice to be somewhat sharpened. The factor in question arises in the evaluation of the encounter integrals (see, for instance, Rosenbluth, MacDonald, and Judd 1957). The integrals diverge mathematically; hence physically one cuts them off at an upper limit, which is now recognized (Cohen, Spitzer, and Routly 1950) to be the distance out to which the star density is the same in all directions. If this distance is called $D_m$, then the argument of the logarithm is

$$\alpha = D_m \langle v^2 \rangle / 2Gm. \tag{34}$$

Since $\langle v^2 \rangle = 3/2j^2$, application of Eq. (15) gives

$$\alpha = \tfrac{2}{3}\pi \nu_0 D_m r_c^2. \tag{35}$$

A good measure for the distance scale of density changes in our models is the core radius; hence we set $D_m = r_c$, so that

$$\alpha = \tfrac{2}{3}\pi \nu_0 r_c^3. \tag{36}$$

Thus $n$ in Eq. (33) can be interpreted as an effective number of stars in the core of the cluster—specifically the number of stars in a homogeneous sphere of radius $r_c$ and density $\nu_0$.

In Paper II, Tables I–X gave values of $\lambda$ as a function of the mass ratio—here equal to unity—and the cutoff velocity $x_e = jv_e$. But according to Eqs. (5) and (9), the value of $x_e^2$ at any point of a cluster model is simply $W$. The eigenvalues $\lambda$ depend strongly on $W$; in fact it can be verified that the values for unit mass ratio are well approximated by the formula

$$\lambda = 4.95 e^{-W}. \tag{37}$$

[This is very similar to Eq. (19) of Paper II.] From $W = 3$ to $W = 10$ this formula is correct within 10%.

Consideration of Eq. (37) shows that the escape rate from a star cluster depends strongly on its central concentration. The higher the central concentration, the larger the central value of $W$, and consequently the smaller the central value of $\lambda$. If two clusters have identical cores—and hence identical central values of $T_R$—the cluster with a more extended envelope will lose stars much more slowly. This behavior makes good sense physically, from either of two points of view. First, a low-concentration cluster is one in which tidal influences reach far in; hence stars find it easier to escape. Second, a spatially extended envelope corresponds to a long tail on the velocity distribution. Such a distribution is already close to Maxwellian, hence further relaxation causes changes that are quantitatively only small ones.

Equation (37) shows that not only does $\lambda$ vary from one cluster model to another; within a given model it varies with position. So also does $T_R$; in this case the variable factor is the number density $\nu$, which is of course equal to $\rho/m$. In the expression for density, Eq. (11), when $W$ is large the integral tends to the constant value $\Gamma(\frac{5}{2})$, with the result that $\rho \propto e^W$. The reference time is then proportional to $e^{-W}$, and the ratio $\lambda/T_R$ in Eq. (32) is independent of position. That is, every part of the cluster loses the same fraction of its stars per unit time.

Strictly speaking, this conclusion applies only to large values of $W$. In fact, however, direct examination of numerical values shows that within a given model $\lambda/T_R$ is 20% higher at $W = 3$ than at $W = 10$—a span over which $\lambda$ and $T_R$ individually vary by a factor of 1000. For smaller values of $W$ this constancy breaks down—but so does our entire mechanism for calculating escape rates. The velocity distribution given by Eq. (7) is no longer a good approximation to the steady-state distribution; and, more fundamentally, the actual relaxation process is no longer well approximated by the simplification of using a Gaussian velocity distribution for the stars encountered. The best one can say is that the conclusion $\lambda/T_R = \text{const}$ has the same range of validity as the basic theory.

Within this range of validity the cluster models are thus dynamically self-consistent in a much stronger way than might originally have been anticipated. The only assumption made was that the velocity distribution satisfies the steady-state Fokker–Planck equation locally at the center of the cluster. It thereupon turned out that the corresponding velocity distributions gratuitously satisfied this equation everywhere else in the cluster. Furthermore, the fractional loss rate has turned out to be everywhere the same, so that the loss of stars does not cause any immediate change in the shape of the density distribution.

One cannot argue that these models are completely steady, however. The loss of stars causes a change in the cluster's gravitational field, and a density readjustment ensues. On this largest scale, in fact, no strictly steady state is possible at all. The equation that describes the entire cluster—the Liouville equation with Fokker–Planck terms appended—is a mixture of terms of first and second degree, and the variables thus cannot be separated. What the cluster presumably does, however, is to settle down into a state that is as close as possible to steady, thereupon evolving quasi-statically through a sequence of such states. The regularities found observationally in Paper I indicate that such a sequence exists, while the observational and theoretical arguments given in the present paper suggest that the real sequence resembles the sequence of models described above.

## VII. DYNAMICAL EVOLUTION

If we assume the existence of a unique sequence of cluster models, then the evolution of an individual cluster can be followed as it progresses down the sequence. The loss of stars causes (a) a decrease in the mass $M$, (b) a decrease in $r_t$, which is proportional to $M^{\frac{1}{3}}$, and (c) a calculable change in the total energy of the cluster. The problem is then simply to find the model that fits the changed values of $M$, $r_t$, and the total energy $H$.

For this purpose the mass and potential energy were calculated for each of the present models. The quantities calculated were

$$\mu=\int_0^{R_t}\frac{\rho}{\rho_0}4\pi R^2dR \tag{38}$$

and

$$\beta=\int_0^{R_t}W\frac{\rho}{\rho_0}4\pi R^2dR, \tag{39}$$

where $R_t$ is of course the same as the central concentration $c=r_t/r_c$. The actual mass is clearly

$$M=\rho_0 r_c^3\mu. \tag{40}$$

The actual potential energy is somewhat more complicated; first, integrating the potential with respect to mass gives twice the potential energy, since every interaction is thus counted twice. Hence the potential energy is

$$U=\frac{1}{2}\int_0^{r_t}4\pi V'\rho r^2dr, \tag{41}$$

where $V'$ is the true potential, equal to zero at infinity. In the model calculation a shifted potential $V$ was used, however, with its zero at $r=r_t$, at which point $V'=-GM/r_t$. Hence

$$V=V'+GM/r_t. \tag{42}$$

With the use of Eqs. (9), (13), (15), (38)–(40), and (42), Eq. (41) now becomes

$$U=-(k+\tfrac{1}{2})GM^2/r_t, \tag{43}$$

where

$$k=(2\pi/9)\beta c/\mu^2. \tag{44}$$

Values of $c$, $\mu$, $\beta$, and $k$ are given in Table II for various values of $W_0$.

The change in the cluster's energy results from the tidal assistance given to the escape of stars. In the present idealization of tidal effects, the tidal force does not affect the interior of the cluster; it simply removes any star that reaches the tidal limit. The tidal force thus contributes an energy

$$dH=-(GM/r_t)dM \tag{45}$$

Table II. Characteristics of cluster models.

| $W_0$ | $c$ | log$c$ | $\mu$ | $\beta$ | $k$ | $1/\lambda$ | $\lambda\mu^{\frac{1}{2}}c^{\frac{3}{2}}$ |
|---|---|---|---|---|---|---|---|
| 2.5 | 3.891 | 0.590 | 3.934 | 5.553 | 0.97 | 2.083 | 7.30 |
| 3 | 4.699 | 0.672 | 5.182 | 8.721 | 1.07 | 3.703 | 6.25 |
| 4 | 6.920 | 0.840 | 8.102 | 17.81 | 1.31 | 11.03 | 4.71 |
| 5 | 10.70 | 1.029 | 11.81 | 31.34 | 1.68 | 31.40 | 3.83 |
| 6 | 17.99 | 1.255 | 16.90 | 50.73 | 2.23 | 87.42 | 3.59 |
| 7 | 33.71 | 1.528 | 24.93 | 78.90 | 2.98 | 240.4 | 4.06 |
| 8 | 68.15 | 1.833 | 39.89 | 122.5 | 3.66 | 657.2 | 5.41 |
| 9 | 131.4 | 2.119 | 69.89 | 195.7 | 3.67 | 1791 | 7.04 |
| 10 | 223.7 | 2.350 | 125.7 | 324.2 | 3.20 | 4874 | 7.68 |
| 12 | 548.2 | 2.739 | 369.2 | 927.5 | 2.60 | | |
| 15 | 2272 | 3.356 | 1576 | 4246 | 2.71 | | |

to the escaping mass $-dM$. Since the virial theorem states that $H=\frac{1}{2}U$, Eqs. (43) and (45) give

$$dU/U=2dM/(k+\tfrac{1}{2})M, \tag{46}$$

and differentiation of Eq. (43), with $r_t\propto M^{\frac{1}{3}}$, leads to

$$dk/dM=(-10k+7)/6M. \tag{47}$$

Rearrangement of Eq. (47) in the form

$$d(k-0.7)/dM=-(5/3)(k-0.7)/M \tag{48}$$

then shows that for a cluster subject only to tidal forces and internal relaxation the quantity $k-0.7$ varies as $M^{-5/3}$. Since for all reasonable cluster models $k$ is greater than 0.7, this means that $k$ must increase as $M$ decreases. The change in $k$ gives, via Table II, the change in central concentration, as measured by either the theoretical $W_0$ or the observational $c$.

The exact functional dependence of $k$ on $M$ must not, however, be taken seriously, since this simple treatment has omitted other dynamical phenomena that affect the energy balance of the cluster—particularly mass loss from stellar evolution and tidal shocks due to passing large masses. Both these phenomena add energy to the cluster and tend to counteract the contractive tendency just found. For any specific cluster these energy effects must be added into an equation similar to Eq. (46); the result, corresponding to Eq. (47), will show whether $k$ increases or decreases, depending on the relative sizes of the various effects. The general conclusion, in any case, is that the central concentration of the cluster will change in a way that is determined by the energy balance; the nature of the change can be found by a procedure of the sort demonstrated.

A related question is how the rate of evolution of the cluster will change as stars are lost. According to the traditional picture of cluster evaporation (Gurevich and Levin 1950; King 1958; von Hoerner 1958) any contraction of the cluster will sharply speed its loss of stars, since the contraction greatly shortens the relaxation time. The present models show this conclusion to be incorrect, however, because of the large compensating changes in $\lambda$. To see this, we show, in as clear a way as possible, how $W_0$ affects the escape rate

$\lambda/T_R$. Combination of Eqs. (33), (15), and (40) gives

$$T_R^{-1} = (27/8)(G/2\pi)^{\frac{1}{2}} m \ln(\tfrac{1}{2}n_c)(\mu/M)^{\frac{1}{2}} r_c^{-\frac{3}{2}}, \quad (49)$$

where $n_c$ was shown in the preceding section to be the number of stars in the central core of the cluster. The individual mass $m$ can now be written $M/n$ and the limiting radius introduced via

$$r_t = (M/\kappa)^{\frac{1}{3}}. \quad (50)$$

The constant $\kappa$ expresses the strength of the tidal force; for a globular cluster

$$\kappa = 3.5 M_g / R_p^3 \quad (51)$$

(Paper I, Sec. III), where $M_g$ is the effective attracting mass of the Galaxy and $R_p$ is the cluster's distance of closest approach to the galactic center. For an open cluster

$$\kappa = 4\omega A/G, \quad (52)$$

where $\omega$ is the angular velocity of rotation and $A$ is the first Oort constant. Elimination of $m$ and substitution for $M$ from Eq. (50) now give Eq. (49) the form

$$\lambda/T_R = (27/8)(G/2\pi)^{\frac{1}{2}} \kappa^{\frac{1}{2}} n^{-1} \ln(\tfrac{1}{2}n_c)\lambda\mu^{\frac{1}{2}} c^{\frac{3}{2}}, \quad (53)$$

where $\lambda$ is to be evaluated at the cluster center. The loss rate thus depends on the number of stars, the strength of the tidal force, and $\lambda\mu^{\frac{1}{2}}c^{\frac{3}{2}}$, which is a pure function of $W_0$. For the range of concentrations covered by star clusters, the last column of Table II gives values of $\lambda\mu^{\frac{1}{2}}c^{\frac{3}{2}}$, which can be seen to depend very little on $W_0$. Thus during the evolution of a cluster the rate of loss of stars changes very little with time.

This constancy of loss rate has, in fact, an even greater generality. Eq. (53) is not restricted to the evolution of a single cluster; it applies to any cluster at any time. Thus within a wide range of central concentrations the escape rate of stars from a cluster depends only on the number of stars and the tidal field in which the cluster finds itself. There is no obvious physical reason for this simplicity; it seems to arise from a fortuitous compensation of opposing effects.

Some further interesting conclusions can be drawn from Eq. (48) and the values of $k$ in Table II. First, the model changes rapidly as stars are lost. In the middle range of central concentrations a loss of about 25% of the stars will cause $W_0$ to increase by 1. (Stellar mass loss and tidal shocks will reduce this rate, however, and may even reverse it.) Second, for central concentrations somewhat lower than the lowest observed, $k$ will become less than 0.7 and the escape of stars will have an expansive effect. For such a cluster all evolutionary processes are expansive; the cluster presumably grows until it becomes completely unstable tidally.

The third conclusion follows from the behavior of $k$ at high $W_0$. The potential energy parameter $k$ reaches a maximum for a value of $W_0$ between 8 and 9; thereafter it oscillates and approaches (as shown by computations of models up to $W_0 = 30$) an asymptotic value that appears to be equal to $8\pi/9$, or 2.793. In this range of high central concentration an evolving cluster cannot continue to satisfy Eq. (48). Physically speaking, both the mass and the potential energy are now determined almost completely by the envelope, and no further changes in the core will make any appreciable difference. It might currently be fashionable to predict the consequent collapse of the core, but it is more reasonable instead to expect a readjustment of the envelope in such a way as to make the potential energy more strongly negative. It thus appears that for the highest central concentrations the models discussed here can no longer be the correct evolutionary sequence—although the profiles of elliptical galaxies suggest that the difference is not great. The difference may result from anisotropy of the velocity distribution—which would steepen the density gradient in the right sense—or it may require a more basic revision of the theory.

## VIII. SUMMARY

From the foregoing discussions a picture emerges of the basic dynamics of star clusters. The dominant process is relaxation, which brings the internal velocity distribution close to a Gaussian form. As a result the central cores of all clusters have identical profiles, except for the obvious scale factors of radius and star number. The envelope of a cluster, by contrast, is molded by the tidal force in which the cluster finds itself. Specifically, the profile of the envelope is determined by the ratio of the tidal limiting radius to the core radius—a quantity that may be referred to as the central concentration. Except for scale factors, clusters differ only in central concentration.

The spatial limitation corresponds to a cutoff in the velocity distribution, at a velocity less than that of escape to infinity. Continuing relaxation and escape make the velocity distribution a near-Gaussian steady-state solution of the Fokker–Planck equation. Velocity distributions of this type correspond spatially to modified isothermal spheres, with the central concentration related to the location of the velocity cutoff. These models have density profiles that resemble those observed in open clusters, where the central concentrations are always low, and globular clusters, where the concentrations range from low to high. Elliptical galaxies also appear to fit the same models, even though their relaxation times are too long to account for the similarity.

A modified isothermal model is very nearly stationary overall. Not only is the velocity distribution steady at the cluster center; it is steady everywhere, and the fractional loss rate is the same everywhere. Evolution occurs only as a reaction to the decreasing total number of stars. The observed prevalence of these models suggest that evolution is along the sequence that they represent. At the very highest central concentrations,

however, the sequence probably fails to represent actual physical systems correctly.

The rate of escape of stars follows directly from the models. An extensive envelope inhibits escape, but a small core speeds relaxation. The two effects tend to compensate, resulting in an escape rate that depends on the number of stars in the cluster and the strength of the tidal field but is almost independent of central concentration. It follows as a corollary that the escape rate changes very little with time.

As time passes, the central concentration of a cluster changes in a way that is determined by gains and losses of energy. Escape of stars makes the core contract, while encounters with interstellar clouds and mass loss from stellar evolution both cause it to expand. The balance between these contractive and expansive forces determines the direction and rate of evolution.

These are the general dynamical properties of star clusters, as they follow from the arguments given in this paper. Their application depends, however, on the use of realistic mixed models, fitted to observations of actual clusters. Later papers of this series will continue in that direction.

## ACKNOWLEDGMENTS

Throughout its course this work has been supported by grants from the National Science Foundation. Part of the work was carried out while I enjoyed the hospitality of Mount Wilson and Palomar Observatories. The calculations were carried out on computers at the California Institute of Technology, the University of Illinois, and the University of California at Berkeley.

## REFERENCES

Chandrasekhar, S. 1943a, *Revs. Mod. Phys.* **15**, 1.
——. 1943b, *Astrophys. J.* **98**, 54.
——. 1960, *Principles of Stellar Dynamics* (Dover Publications, Inc., New York).
Cohen, R. S., Spitzer, L., and Routly, P. McR. 1950, *Phys. Rev.* **80**, 230.
Gurevich, L. E., and Levin, B. J. 1950, *Dokl. Akad. Nauk SSSR* **70**, 781.
Hodge, P. W. 1961a, *Astron. J.* **66**, 249.
——. 1961b, *ibid.* **66**, 384.
——. 1962, *ibid.* **67**, 125.
——. 1964, *ibid.* **69**, 853.
Jeans, J. H. 1915, *Monthly Notices Roy. Astron. Soc.* **76**, 70.
King, I. 1958, *Astron. J.* **63**, 114.
——. 1962, *ibid.* **67**, 471.
——. 1965, *ibid.* **70**, 376.
Michie, R. W. 1963a, *Monthly Notices Roy. Astron. Soc.* **125**, 127.
——. 1963b, *ibid.* **126**, 499.
Michie, R. W., and Bodenheimer, P. H. 1963, *ibid.* **126**, 269.
Miller, R. H., and Prendergast, K. H. 1962, *Astrophys. J.* **136**, 713.
Oort, J. H., and van Herk, G. 1959, *Bull. Astron. Inst. Neth.* **14**, 299 (No. 491).
Rood, H. J. 1965, *Astron. J.* **70**, 689.
Rosenbluth, M. N., MacDonald, W. M. and Judd, D. L. 1950, *Phys. Rev.* **107**, 1.
Spitzer, L., and Härm, R. 1958, *Astrophys. J.* **127**, 544.
Vaucouleurs, G. de. 1959, *Handbuch der Physik*, edited by S. Flügge (Springer-Verlag, Berlin), Vol. 53, p. 311.
von Hoerner, S. 1957, *Astrophys. J.* **125**, 451.
——. 1958, *Z. Astrophys.* **44**, 221.
Woolley, R.v.d.R. 1954, *Monthly Notices Roy. Astron. Soc.* **114**, 191.
——. 1961, *Observatory* **81**, 161.
Woolley, R.v.d.R., and Dickens, R.J. 1961, *Royal Obs. Bull.* No. 42.
Woolley, R.v.d.R., and Robertson, D. 1956, *Monthly Notices Roy. Astron. Soc.* **116**, 288.